Heat Transfer in Cemented Hip Replacement Process

Kamonchat Kaorapapong, Somkid Amornsamankul, I-Ming Tang, Benchawan Wiwatanapataphee

***Abstract*— This paper proposes a mathematical model of heat transfer in the cemented hip replacement using the metal-metal implant with no cup. Computational domain consists of three subregions including a femur region, an implant region and a femoral canal region. The femoral region is divided into two parts which are the top and the bottom parts occupied by the cement and the ambient air. The governing equation is a unsteady heat equation. Heat transfer by conduction is considered in this study. Finite element formula for the solution of heat transfer problem is derived. Effect of the initial temperature of the cement and the implant material on heat transfer process are investigated. Numerical results show that the initial temperature has significant effect whereas the implant materials has less effect.**

***Keywords*— unsteady heat equation, finite element method, cemented hip replacement, mathematical model, femur bone, implant material.**

I. Introduction

A Lot of old people in the world get lost in a movement and become chronic pain patients because of the damaged hip joint and the hip arthritis. Many treatments such as weight loss, walking aids, physical therapy, medications, activity modification, anti-inflammatory, joint supplements (glucosamine), hip resurfacing surgery and hip replacement surgery are used to improve the mobility and release pain. The hip replacement surgery is often used in severe cases. There are two techniques of total hip replacement including the cementing and cementless techniques. Cemented fixation is attached to the existing bone with hot cement, which acts as a glue and attaches the artificial joint to the bone. Ice pack is applied to reduce nuisance and painfulness in the hip area for 20 minutes. Cementless fixation is attached by the total hip prosthesis which pushed directly in the femoral canal and held there by the elastic forced generated in the bone tissue. The patients frequently choose medical treatment by cemented hip replacement because of fast rehabilitation after surgery. Normally, cemented hip replacement has useful life for 10 - 15 years after surgery. The quality of the bone cement interface is important to increase the useful life span of the cemented hip replacement. Even though the total hip replacement has been successfully for many years, implant failure or implant loosening still happens due to the inflection and the incomplete heat transfer in the bone-cement-prosthesis process. Many scientists have tried to understand the complex phenomena involving the cement flow and heat transfer during the hip replacement surgery using mathematical model and numerical simulation. [1], [2], [3], [4], [5], [6], [7], [8], [9], [10], [11], [12], [13], [14], [15].

The stress distribution within the normal and osteoarthritis femur is investigated through the use of two dimensional plane stress finite element analysis by Elkholy et al.(2005, [16]). It is found that at the outer layers of the femur head, there were regions of extremely low stresses where the bone may be atrophy and cause a void formation.

Valliappan et al.(1977, [17]) used a three-dimensional finite element analysis to examine stress of the proximal end of the human femur. They constructed the model of the cortical and cancellous regions as isotropic continua with appropriate bulk elastic properties.

Royi et al.(2005, [18]) studied femur three dimensional finite-element (FE) analysis based on CT data to compute both the accurate geometry representation and mechanical properties assignment. They recommended a structure based method for the reconstruction of a FE model and the geometry was represented by smooth surfaces extracted from the CT data including a separating surface between trabecular regions and cortical. Their method showed good results, compared to voxel-based method.

Krauze et al.(2008, [19]) studied stresses and displacement in femur in a living and a dead phase using numerical analysis. The influence of different mechanical properties of bone tissue was presented.

Oquz and Bulent(2007, [20]) proposed parametric modeling and the effect of body weight load during stumbling on the behavior of newly designed implants was investigated. They found that decreasing the stress on the femur and the bone - cement depend on the factors in the implant design. Therefore, a suitable implant hip prostheses could be constructed and

Manuscript received May 31, 2011; revised May 31, 2011. This research project is supported by Centre of Excellence in Mathematics, CHE, Bangkok, Thailand.

K. Kaorapapong is with Department of Mathematics, Faculty of Science, Mahidol University, Bangkok, Thailand (email: g5237091@student.mahidol.ac.th)

S. Amornsamankul (corresponding author) is with Department of Mathematics, Faculty of Science, Mahidol University, and is with Centre of Excellence in Mathematics, CHE, Bangkok, Thailand (email: scsam@mahidol.ac.th)

I.M. Tang is with ThEP Center, CHE, 328 Si Ayutthaya Road, Bangkok, Thailand (email: scimt@mahidol.ac.th)

B. Wiwatanapataphee is with Department of Mathematics, Faculty of Science, Mahidol University, and is with Centre of Excellence in Mathematics, CHE, Bangkok, Thailand (email: scbww@mahidol.ac.th)

studied with computer modes before implementation to the patient.

Hansen(2005, [10]) developed the model of the heat transfer in a general bone - cement - prosthesis system and founded that the heat transfer and the polymerization kinetics in the system caused the injury to the bone tissue and chemical history of the system. The finite element method was utilized in this model in order to simulate a cross section of a hip with a femoral stem prosthesis. His results from the model indicated that an auto accelerating heat production and a residual monomer concentration were able to cause bone tissue damage and affected the mechanical properties of the cement.

J. Okrajni et al.(2007, [11]) proposed a mathematical model of the heat flow in surgical cement during implantation. Their model describes the temperature distribution in the bone during the surgery treatment.

In this paper, we study heat transfer by conduction on the full part of the femur bone with inserted implant. Three different implant materials including alumina, cobalt chrome and titanium, and three initial cement temperatures of 65 $^{\circ}C$, 80 $^{\circ}C$ and 100 $^{\circ}C$ are used to investigate their impact on the heat transfer problem. The rest of the paper is organized as follows. Section 2 describes mathematical model of the heat transfer problem in the cemented hip replacement process. Finite element formula are presented in section 3. Section 4 concerns the numerical example results of the study. Finally, conclusion is given in section 5.

II. Mathematics Model

In this study we focus on heat transfer by conduction in the cemented hip replacement. Essential region of the cemented hip replacement as shown in Figure 1 consists of a femur region, an implant region and a femoral region. On the top part of femoral region is occupied by the cement and the bottom part is occupied by the ambient air. The governing equation to describe the heat transfer problem is the unsteady heat equation [8]:

$$\rho C_p \frac{\partial T}{\partial t} + \nabla \cdot (-k \nabla T) = 0, \text{ in } \Omega \times I \tag{1}$$

where T is temperature field, ρ is the density, C_p is the heat capacity at constant pressure, k is the thermal conductivity and t represents time in second and $I = [0, \tau]$ is the time interval. Values of model parameters for each region are presented in Table I.

To completely define the problem, boundary conditions need to be specified. On the surface of the head of the implant Γ_{head}, the outer surface of the femur Γ_{fem} and the inlet surface of cement Γ_{cem}, Newton boundary condition [21] is applied, i.e.,

$$-k_i \frac{\partial T^i}{\partial \mathbf{n_i}} = h^i_{\infty}(T^i - T^{ext}), \ i = 1, 2, 3 \tag{2}$$

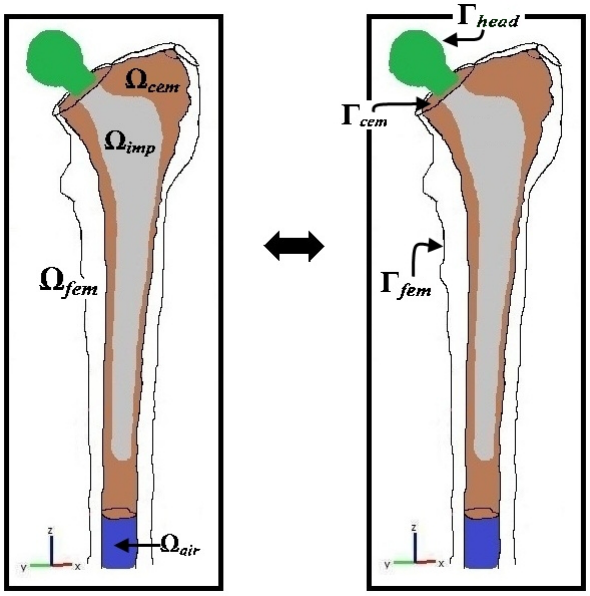

Fig. 1. Four sub domains and boundaries of the femur bone.

where the index i refers to the i^{th} region where $i = 1, 2$ and 3 for the femur surface (Γ_{fem}), the head of implant surface (Γ_{head}) and the cement surface (Γ_{cem}). T_i andh^i_{∞} denote an unknown surface temperature and heat transfer coefficient for each material, respectively. $\mathbf{n_i}$ denotes the outward unit normal to Γ_i.

On the interfaces between any two regions, we impose the continuity of the heat flux across the contact surface, i.e.,

$$k_i \frac{\partial T^i}{\partial \mathbf{n_i}} - k_j \frac{\partial T^j}{\partial \mathbf{n_j}} = 0. \tag{3}$$

In summary, heat transfer process after the cemented hip replacement is governed by the parabolic partial differential equation (1) with boundary value problems (BVP) (2, 3) and initial condition (I.C.) which is the parabolic boundary values problems (BVP).

Parabolic BVP : Find $T \in \Omega \times I$ such that the parabolic partial differential equation (1) with boundary conditions (2) and (3) and initial condition (I.C.) are satisfied.

$$\rho C_p \frac{\partial T}{\partial t} + \nabla \cdot (-k \nabla T) = 0, \Omega \times I$$

Subject to B.C.

$$\begin{aligned} -k_i \frac{\partial T^i}{\partial \mathbf{n_i}} &= h^i_{\infty}(T^i - T^{ext}), i = 1, 2, 3, \\ k_i \frac{\partial T^i}{\partial \mathbf{n_i}} - k_j \frac{\partial T^j}{\partial \mathbf{n_j}} &= 0. \end{aligned}$$

TABLE I
THE EXPERIMENT PARAMETERS USED IN THE NUMERICAL SIMULATION OF ARTIFICIAL DOMAIN OF THE FEMUR BONE, AMBIENT AIR, CEMENT, ALUMINA, COBALT IMPLANT, CHROME IMPLANT AND TITANIUM IMPLANT.

Parameters	Femur	Ambient air	Cement	Co-Cr Imp	Al Imp	Ti Imp	Units
Density (ρ)	1000	1.8677	1100	8300	3980	4400	kg/m^3
Thermal conductivity (k)	0.26	0.0398	0.17	13	30.4	6.7	$W/(m \cdot K)$
Heat capacity (C_p)	1260	1557.75	1460	420	800	530	$J/(kg \cdot K)$

Initial condition,

$$T(x,0) = \hat{T}(0) \text{ in, } \Omega$$

where $I = [0, \tau]$.

III. FINITE ELEMENT FORMULATION

To solve the BVP numerically by the finite element method, we multiply equation (1) by a weighting function $v(x)$, then set the total weighted residual error to zero, i.e,

$$\int_\Omega v\rho C_p \frac{\partial T}{\partial t} d\Omega - \int_\Omega v\nabla \cdot (k\nabla T) d\Omega = 0. \tag{4}$$

Using the symmetry of $\nabla \cdot (vk\nabla T)$, we have

$$v\nabla \cdot (k\nabla T) = \nabla \cdot (vk\nabla T) - k\nabla T \cdot \nabla v. \tag{5}$$

Substituting equation (5) into (4) and using the divergence theorem, we obtain

$$\int_\Omega v\rho C_p \frac{\partial T}{\partial t} d\Omega + \int_\Omega k\nabla T \cdot \nabla v d\Omega = \int_{\partial\Omega} vk \frac{\partial T}{\partial n} ds. \tag{6}$$

Imposing the boundary condition into equation (6) yields

$$\begin{aligned} \int_\Omega v\rho C_p \frac{\partial T}{\partial t} d\Omega &+ \int_\Omega k\nabla T \cdot \nabla v d\Omega + \int_{\partial\Omega} vh_\infty T ds \\ &= \int_{\partial\Omega} vh_\infty T_{ext} ds. \end{aligned}$$

Therefore, the variational statement for the BVP can be stated as follows:

Find $T = T(\mathbf{x}, t) \in H^1(\Omega)$ such that for every $t \in I$

$$\begin{aligned} (T_t, v) + a(T, v) &= L(v) \quad \forall v \in H_0^1(\Omega), \\ T(\mathbf{x}, 0) &= \hat{T}(\mathbf{x}) \end{aligned} \tag{7}$$

where

$$\begin{aligned} (\cdot, \cdot) &\quad \text{represents the inner product,} \\ (T_t, v) &= \int_\Omega v\rho C_p \frac{\partial T}{\partial t} d\Omega, \\ a(T, v) &= \int_\Omega k\nabla T \cdot \nabla v d\Omega + \int_{\partial\Omega} vh_\infty T ds, \\ L(v) &= \int_{\partial\Omega} vh_\infty T_{ext} ds. \end{aligned}$$

Let $H_h^1(\Omega)$ be a finite dimensional subspace of H^1 with basis functions $\{\phi_1, \phi_2, \ldots, \phi_n\}$. Then, the variational problem is approximated by:

Find $T_h(\mathbf{x}, t) \in H_h^1$ such that $T_h(\mathbf{x}, 0) = \hat{T}(\mathbf{x})$ and

$$(\frac{\partial T_h}{\partial t}, v_h) + a(T_h, v_h) = L(v_h), \quad \forall v_h \in H_h^1.$$

In the usual way, we introduce a discretization of Ω as a union of elements Ω_e, i.e, $\Omega \longrightarrow \cup_{e=1}^E \Omega_e$ and approximate $T(\mathbf{x}, t)$ at t by.

$$T = \sum_{j=1}^N \phi_j T_j, \quad v = \sum_{j=1}^N \phi_j v_j. \tag{8}$$

From (7) and (8) and by using the usual finite element formulation, we obtain the system of ordinary differential equations

$$\begin{aligned} \mathbf{M}\dot{\mathbf{T}} + \mathbf{AT} &= \mathbf{F}, \\ T(0) &= \hat{T}, \end{aligned} \tag{9}$$

where

$$\mathbf{M} = (m_{ij}), \quad \text{with } m_{ij} = (\phi_i, \phi_j) = \sum_{e=1}^{E} \int_{\Omega_e} \phi_i \phi_j d\Omega$$

$$\mathbf{A} = (a_{ij}), \quad \text{with } a_{ij} = a(\phi_i, \phi_j) = \sum_{e=1}^{E} \int_{\Omega_e} k \nabla \phi_i \cdot \nabla \phi_j d\Omega + \sum_{e=1}^{E} \int_{\partial\Omega_e} \phi_i h_\infty T ds,$$

$$\mathbf{F} = (f_i), \quad \text{with } f_i = L(\phi_i).$$

To solve the system (9), we use forward difference techniques

$$\frac{dT}{dt}(t) = \frac{T(t + \Delta t_r) - T(t)}{\Delta t},$$

with $O(\Delta t)$ accuracy.

The system (9) then becomes

$$\mathbf{M}\mathbf{T}_{r+1} = (\mathbf{M} - \Delta t_r \mathbf{A})\mathbf{T}_r + \Delta t_r \mathbf{F}_r, \tag{10}$$

where

$$\sum_{r=1}^{n} \Delta t_r = \tau$$

Hence, starting with T_0 at $r = 0$, we can generate a sequence of solutions $T_0, T_1, \ldots, T\tau$ corresponding to $t_1, t_2, \ldots, t_\tau$.

IV. Numerical results

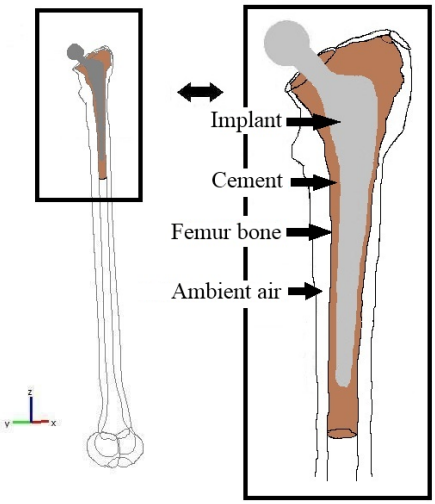

Fig. 2. Geometry of the right artificial femur bone with implant.

The example under consideration is a right artificial femur bone with the length of $50\,cm$. The implant has a length of $15\,cm$. PMMA cement is assumed to be in between the implant and the femur bone and covers the top $17\,cm$ of the femoral canal. Moreover, ice pack covering the leg is used to increase the temperature gradient needed for the decreasing of heat. Three dimensional model of the right artificial femur was constructed based on real domain using a set of CT scan data and Mimics software. The artificial domain as shown in Figure 1 consists of four parts including femur region (Ω_{fem}), the implant region (Ω_{imp}), the cement region (Ω_{cem}) and the ambient region (Ω_{air}). The implant is assumed to be fixed inside femoral canal and is surrounded with cement. Figure 2 shows the complete geometry of the right artificial femur bone with implant.

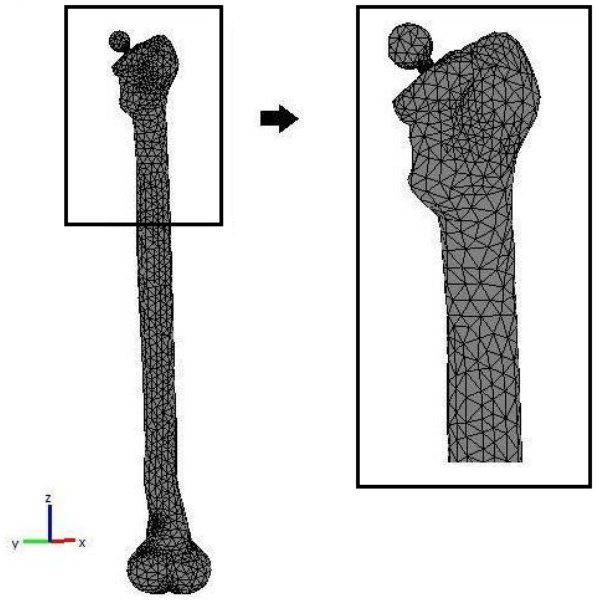

Fig. 3. The finite element mesh ambient air and the top part of computational domain.

The computational domain as shown in Figure 3 is separable in space into 86,493 tetrahedral elements and 126,809 degrees of freedom. Values of model parameters used in the simulation collected from the literature [5], [22], [23], [24], [25], [26] are shown in Table I and Table II. In the numerical simulation, the initial temperatures of femur bone, bone tissue, ambient air, cement and implant were set to be 37 $^\circ C$, 38 $^\circ C$, 35 $^\circ C$, 100 $^\circ C$ and 23 $^\circ C$, respectively.

TABLE II
VALUES OF HEAT TRANSFER COEFFICIENTS FOR EACH MATERIALS, h_∞, $W/(m^2K)$ [26].

	Cement	Ambient
Metal stem	1,000 - 10,000	50 - 100
Femur bone	100 - 1,000	500 - 10,000

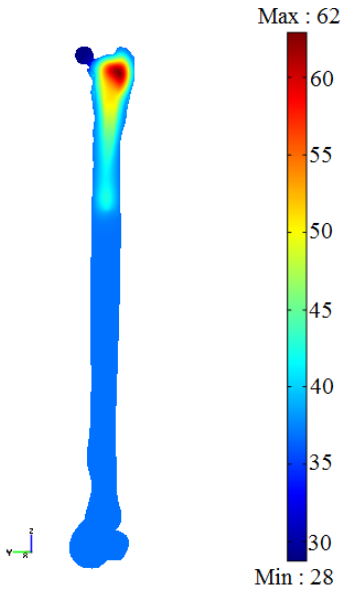

Fig. 4. Temperature distribution on a vertical cross section along the axial artificial domain with the cobalt chrome implant at 360 sec. with initial cement temperature of 100 $^{\circ}C$.

In this study, we focused on the temperature distribution during cooling in the cemented hip replacement process. All temperature values in the computation regions have been computed. The heat transfer from the cement through the implant and from the cement through the bone layers have been investigated. Figure 4 represents the temperature distribution on a vertical cross section along the axial femur bone with cobalt chrome implant at t = 360 sec where high rate of heat transfer is presented. It is founded that in the cement region, temperature between at the bottom of the implant and above the cement plug is about 37 $^{\circ}C$. In the top part of the cement region, maximum temperature is 62 $^{\circ}C$. This show that the high temperature region is presented only in the upper region of the femur.

Figure 5 shows the temperature distribution on three different horizontal cross sections on the top 17 cm of the computational domain. The results indicate that the heat is generated by the hardening of the cement. Heat from the cement transfers to the implant, thereby increases the temperature. This show up by the red color of the whole region in the middle frame. The bottom frame shows that after all the heat has been generated by the hardening of the cement, heat is then lost by the implant first. Heat lost by the cement is lower. That causes the temperature of the cement to be higher than the temperature of the implant seen in the bottom frame.

The middle set of the frame is the temperature distribution at middle of the implant. The top frame here we see the implant appear at the blue color in the middle of the harder cement. The middle frame shows the equilibrium temperature when the temperature of the cement is equilibrium with the implant. In the last frame, we see that the implant is not cool down as fast as the implant in the previous bottom from at the beginning of the implant. The cause of this is that there is no way for the heat to be lost by the implant without the heat passing through the bone. The last frame, there is no implant area presented and only the cement and bone are presented. The cooling is therefore uniform and the temperature is more or less constant.

To investigate the effect of implant material on heat transfer process, three types of implant materials including Alumina, Cobalt Chrome and Titanium are used in the simulation. The results show that temperature profile at point P_2 on the middle part of implant obtained from the model with different implant material are very different whereas there is small difference in temperature profile at the point P_1 on the top part of the implant and the point P_3 on the cement plug as shown in Figure 6. The effect of initial cement temperature on the heat transfer from cement to the bone is investigated for three different implant materials. It is noted that the implant cement temperature has significantly effect. Higher initial temperature gives high rate of the heat transfer from cement to the bone as shown in Figure 7.

V. Conclusion

A mathematical model of heat transfer in the cement hip replacement has been developed to study heat transfer by conduction in the femur bone. Numerical simulation is carried out to investigate the effect of the initial temperature of the cement and the implant material on heat transfer process. It is noted that the initial temperature has significant effect on the heat transfer from the cement in the femoral canal to the surrounding bone. The effect of implant material used in the model is also investigated. The result show that it has less effect on the heat transfer process.

Acknowledgment

Kaorapapong would also like to thank the Science Achievement Scholarship (SAST).

References

[1] S. Toksvig-Larsen, H. Franzen, and L. Ryd, "Cement interface temperature in hip arthroplasty," *Acta Orthopaedica Scandinavica*, vol. 62, pp. 102–105, 1991.

[2] A. Maffezzoli, D. Ronca, G. Guida, I. Pochini, and L. Nicolais, "In-situ polymerization behaviour of bone cements," *Journal of Mater Science Mater Medicine*, vol. 8, pp. 75–83, 1997.

[3] A. Borzacchiello, L. Ambrosio, L. Nicolais, E. Harper, K. Tanner, and W. Bonfield, "Comparison between the polymerization behavior of a new bone cement and a commercial one: modeling and in vitro analysis," *Journal of Materials Science Materials in Medicine*, vol. 9, pp. 835–838, 1998.

[4] D. Ikeda, M. Saito, A. Murakami, T. Shibuya, K. Hino, and T. Nakashima, "Mechanical evaluation of a bio-active bone cement for total hip arthroplasty," *Medical and Biological Engineering and Computing*, vol. 38, pp. 401–405, 2000.

[5] G. Bergmann, F. Graichen, A. Rohlmann, N. Verdonschot, and G. Lenthe, "Frictional heating of total hip implants. part 2: finite element study," *Journal of Biomechanics*, vol. 34, no. 4, pp. 429–435, April 2001.

[6] C.-C. Hu, J.-J. Liau, C.-Y. Lung, C.-H. Huanga, and C.-K. Cheng, "A two-dimensional finite element model for frictional heating analysis of total hip prosthesis," *Materials Science and Engineering*, vol. 17, pp. 11–18, 2001.

[7] N. J. Dunne and J. F. Orr, "Curing characteristics of acrylic bone cement," *Journal of materials science: materials in medicine*, vol. 13, pp. 17–22, 2002.

[8] E. Hansen, "Modelling heat transfer in a bone-cement-prosthesis system," *Journal of Biomechanics*, vol. 36, pp. 787–795, 2003.

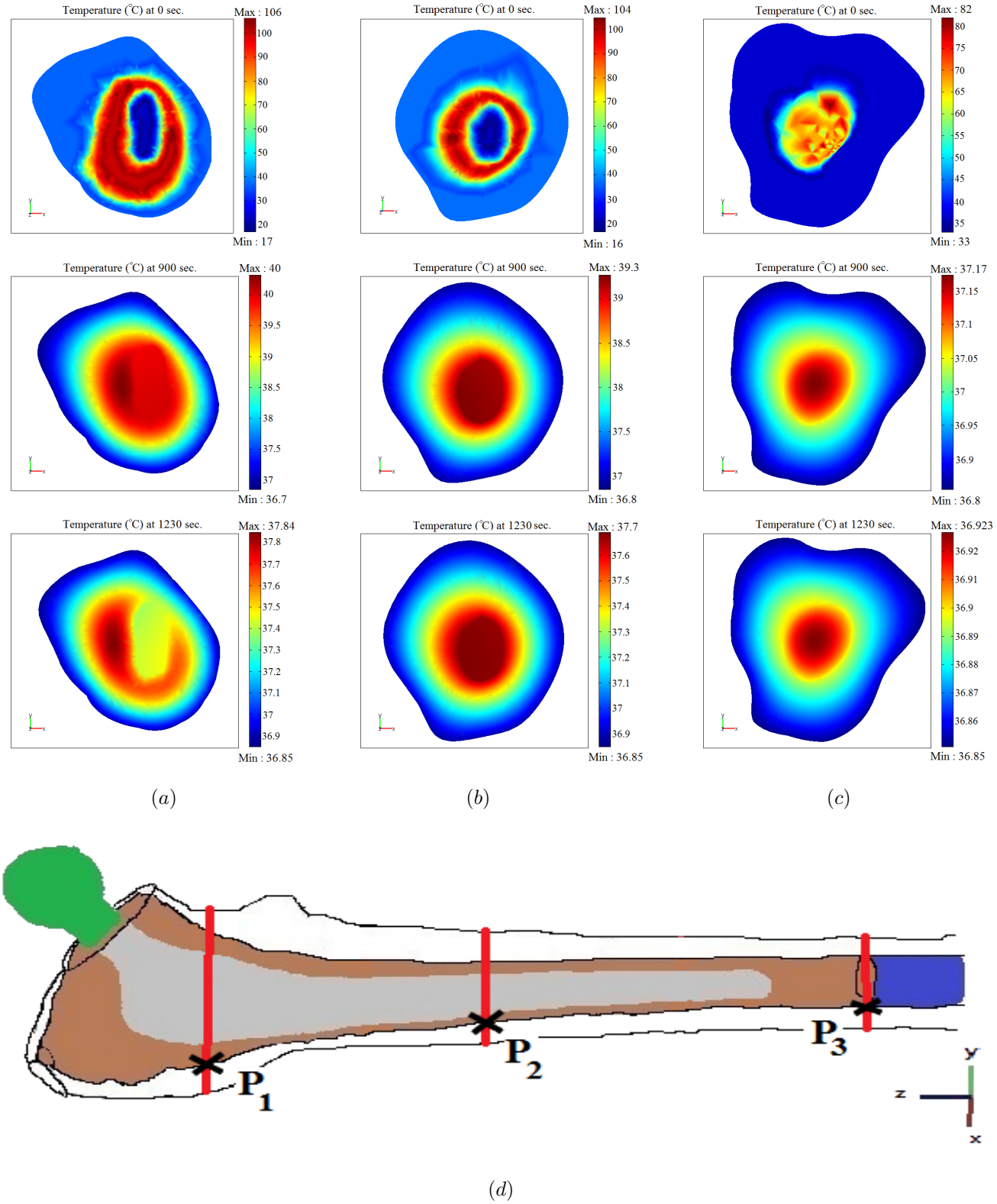

Fig. 5. Temperature distribution at initial stage t = 0 sec., at middle stage t = 900 sec. and the end t = 1230 sec. on three horizontal cross sections; (a) the top part of implant stem, (b) the middle part of implant stem and (c) the cement plug.

[9] W. Walsh, M. Svehla, J. Russell, M. Saito, T. Nakashima, R. Gillies, W. Bruce, and R. Hori, "Cemented fixation with pmma or bis-gma resin hydroxyapatite cement: effect of implant surface roughness," *Biomaterials*, vol. 25, pp. 4929–4934, 2004.

[10] H. Eskil, "Modelling heat transfer in a bone-cement-prosthesis system," *Journal of Biomechanics*, vol. 36, no. 6, pp. 787–795, 2005.

[11] J. Okrajni, M. Plaza, and S. Ziemba, "Computer modelling of the heat flow in surgical cement during endoprosthesoplasty," *Journal of Achievements in Materials and Manufacturing Engineering*, vol. 20, pp. 1–22, January-February 2007.

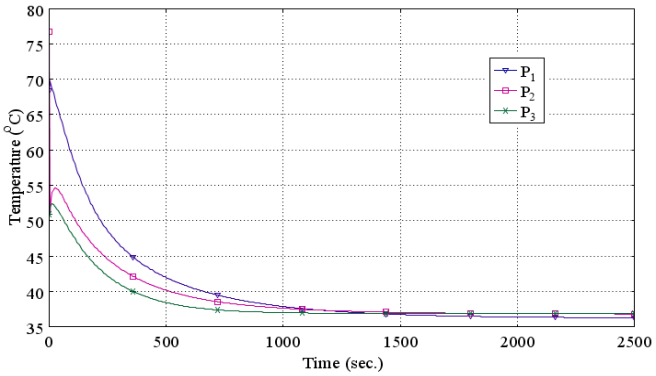

(a) Cobalt chrome implant.

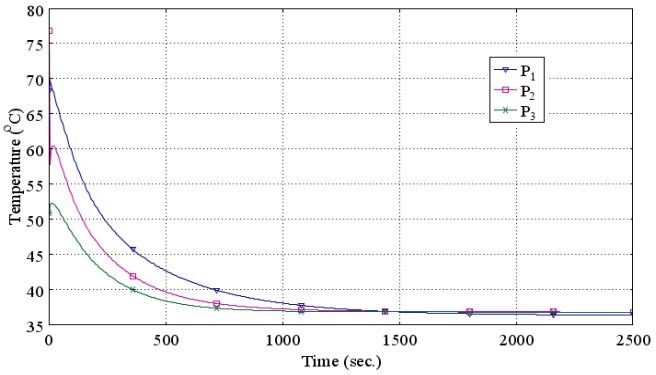

(b) Titanium implant.

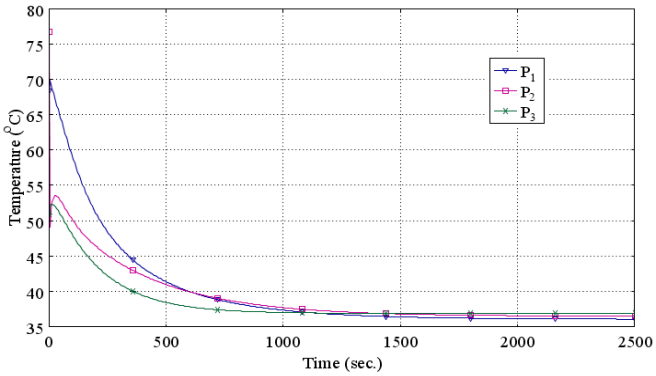

(c) Alumina implant

Fig. 6. Temperature profile at three different points(P_1, P_2 and P_3 as shown in Figure 5) on the cement-femur interface of three horizontal cross sections with three different implant materials including; (a) cobalt chrome implant, (b) titanium implant and (c) alumina implant.

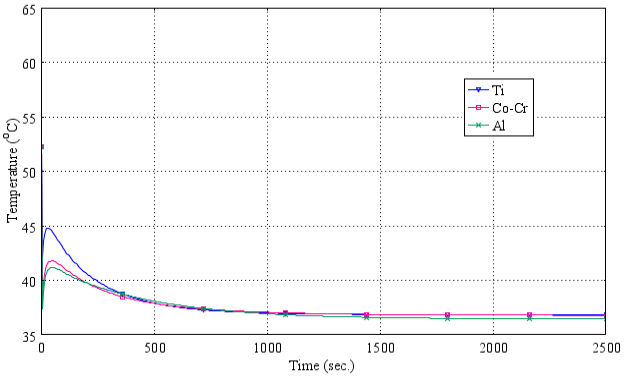

(a) Initial cement temperature of 65 $^{\circ}C$.

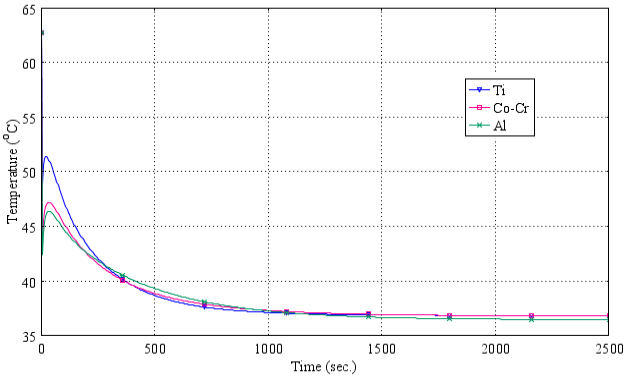

(b) Initial cement temperature of 80 $^{\circ}C$.

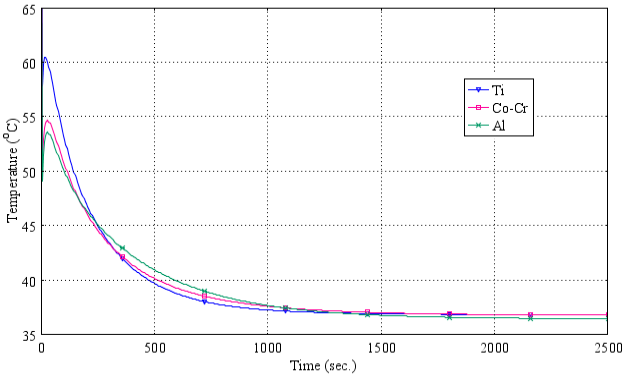

(c) Initial cement temperature of 100 $^{\circ}C$.

Fig. 7. Profile of the cement temperature at a point P_2 obtained from the model with implant temperature of 23 $^{\circ}C$, femur bone of 37 $^{\circ}C$, bone tissue of 38 $^{\circ}C$, ambient air of 35 $^{\circ}C$ and three different values of initial temperature of cement: (a) 65 $^{\circ}C$; (b) 80 $^{\circ}C$ and (c) 100 $^{\circ}C$, respectively.

[12] M. A. Pérez, N. Nuno, A. Madrala, J. M. García-Aznar, and M. Doblar, "Computational modelling of bone cement polymerization: temperature and residual stresses," *Computers in Biology and Medicine*, vol. 39, pp. 751–759, 2009.

[13] C. Precup, A. Naaji, C. Toth, and A. Toth, "Software simulation for femur fractures in case of frontal car accidents," *WSEAS Transactions on Computers*, vol. 7, no. 7, pp. 1050–1060, July 2008.

[14] V. Volpe, C. Miraglia, L. Esposito, and M. Fraldi, "X-ray based technique for estimating bone fracture risk," in *Proceedings of the 2nd WSEAS International Conference on Biomedical Electronics and Biomedical Informatics*, Moscow, Russia, 2009, pp. 244–246.

[15] M. Pawlikowski, "Computer simulation of bone adaptation process under various load cases," in *Proceedings of the 2006 WSEAS Int. Conf. on cellular and molecular biology, biophysics and bioengineering*, Athens, Greece, 14-16 July 2006, pp. 117–122.

[16] E. AH, G. DN, D. FS, and K. MS, "Stress analysis of normal and osteoarthritic femur using finite element analysis," *International Journal of Computer Applications in Technology*, vol. 22, no. 4, pp. 205–211, 2005.

[17] V. S, S. NL, and W. RD, "Three dimensional stress analysis of the human femur," *Computers in Biology and Medicine*, vol. 7, pp. 253–264, 1977.

[18] R. Fedida, Z. Yosibash, C. Milgrom, and L. Joskowicz, "Femur mechanical simulation using high-order fe analysis with continuous mechanical properties," Lisbon in Portuga, 2005.

[19] K. A, K. M, and M. J, "Numerical analysis of femur in living and dead phase," *Journal of Achievements in Materials and Manufacturing Engineering*, vol. 26, 2008.

[20] O. Kayabasi and B. Ekici, "The effects of static, dynamic and fatigue behavior on three-dimensional shape optimization of hip prosthesis by finite element method," *Materials and Design*, vol. 28, pp. 2269–2277, 2007.

[21] G. Nikishkov and P. Gennadiy, *Programming Finite Elements in Java*,

1st ed. Springer, 2010.
[22] S. Biyikli, M. Modest, and R. Tarr, "Measurements of thermal properties for human femora," *Journal of Biomedical Materials Research*, vol. 20, no. 9, pp. 1335–1345, Nov - Dec 1986.
[23] R. Clattenburg, J. Cohen, S. Conner, and N. Cook, "Thermal properties of cancellous bone," *Journal of Biomedical Materials Research*, vol. 9, no. 2, pp. 169–182, Mar 1975.
[24] R. Huiskes, "Some fundamental aspects of human joint replacement. analyses of stresses and heat conduction in bone-prosthesis structures," *Acta Orthop Scand Suppl.*, vol. 185, pp. 1–208, 1980.
[25] S. Mazzullo, M. Paolini, and C. Verdi, "Numerical simulation of thermal bone necrosis during cementation of femoral prostheses," *Journal of Mathematical Biology*, vol. 29, no. 5, pp. 475–494, 1991.
[26] M. Stańczyk and J. Telega, "Modelling of heat transfer in biomechanics a review part ii. orthopaedics," *Acta of Bioengineering and Biomechanics*, vol. 4, no. 2, 2002.